Frequency locking to the center of a 532 nm iodine absorption line by using stimulated Brillouin scattering from a single-mode fiber

E. W. Eloranta and I. A. Razenkov

University of Wisconsin—Madison, 1225 West Dayton Street, Madison, Wisconsin 53706

Received September 1, 2005; revised September 23, 2005; accepted September 26, 2005; posted November 11, 2005 (Doc. ID 64572)

A simple method for frequency locking a frequency-doubled Nd:YAG laser to the center of line 1109 of the iodine absorption spectrum is described. The 31.6 GHz frequency shift provided by stimulated-Brillouin scattering from a single-mode silica fiber provides a probe signal that lies on the edge of line 1105 of the iodine spectrum. We adjust the frequency of the laser to maintain the transmission of a 5 cm iodine absorption cell at a value that places the unshifted laser line in the center of line 1109. © 2006 Optical Society of America

OCIS codes: 140.3570, 280.3640.

Iodine absorption lines are often used as blocking filters in laser experiments. High spectral resolution lidars (HSRL) use I_2 absorption cells to separate light that is backscattered by molecules from light that is backscattered by particulates.[1–3] Filtered Rayleigh flow field visualization and Raman and Brillouin scattering experiments use iodine filters to suppress parasitic scattered light from windows and optical elements.[4–6] These applications require that the laser wavelength be locked to the center of an I_2 absorption line.

Frequency locking is typically accomplished by monitoring the transmission of an I_2 reference cell. The need to maintain the laser wavelength at the transmission minima complicates the locking procedure. If a direct measurement of the absorption is used, deviations in either direction from the minima provide an increased transmission, and no sign information is available for the servocorrection signal. This can be overcome by dithering the laser frequency and searching for the minima. However, the dither imposes an undesirable frequency variation. In addition, the precision of the frequency lock is limited because near the minima the cell transmission changes slowly with frequency deviations. Several approaches have been used to overcome these problems.

Precise locking can be achieved by means of Doppler-free spectroscopy; Arie *et al.*[7] achieved errors of ~650 Hz or 2.3×10^{-12}. While this approach has been used in a HSRL,[3] it adds complexity, and, because each absorption feature is composed of several hyperfine lines, it is necessary to ensure that the system is locked to the correct transition.

A simpler frequency-locking system has been achieved by using FM spectroscopy. Arie and Byer[8] demonstrated a frequency stability of better than 2×10^{-11}. An electro-optical phase modulator, high-frequency oscillator, and rf mixer are required in order to implement this system.

Yokoyama *et al.*[9] demonstrate frequency locking by using an acoustic modulator to derive the first derivative of the I_2 absorption. This provides 60 min stabilities of 2.4×10^{-8} or frequency stabilities of ~13 MHz.

It is easier to lock to the edge of an absorption line than to the center of the line. When locking to the edge of a line, frequency deviations from the lock point create error signals that change sign depending on whether the frequency is above or below the lock point. This allows the use of simple servoalgorithms. Furthermore, the absorption varies rapidly with frequency, providing a large error signal for small frequency deviations. Our HSRL[1,10] systems use line 1109(18 787.8098 cm^{-1}) of the I_2 absorption spectrum[11] as a filter to separate molecular scattering from particulate scattering. The laser frequency must be held within 100 MHz of line center and thus requires a frequency stability of $\sim2\times10^{-7}$. Fortuitously, when the laser is tuned to the center of line 1109, the stimulated Brillouin backscattering from a single-mode optical fiber produces a probe signal that lies on the edge of line 1105(18 786.7727 cm^{-1}). Figure 1 shows the I_2 spectrum computed using code published by Forkey.[12] Vertical lines mark the desired lock point in the center of line 1109 and the nominal frequency offset for stimulated Brillouin scattering from a pure silica fiber. The 31.6 GHz offset shown was computed assuming an index of refraction of 1.46 at 532 nm and using the speed of

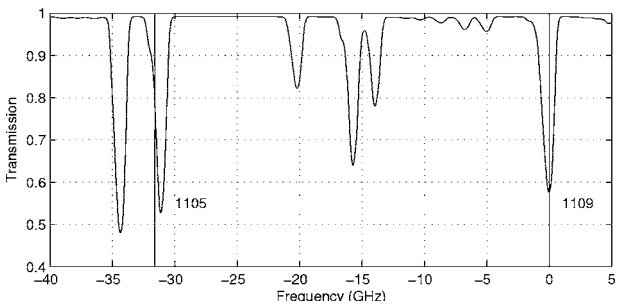

Fig. 1. I_2 spectrum[1] plotted as a function of frequency offset from the center of line 1109 for a 5 cm cell held at 26 °C. Vertical lines mark the center of line 1109 and the frequency offset due to Brillouin scattering computed for a pure silica fiber.

0146-9592/06/050598-3/$15.00

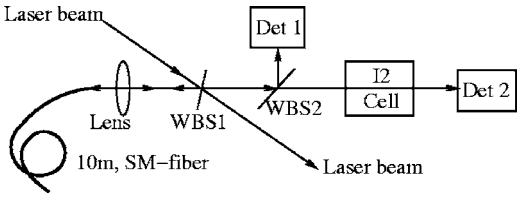

Fig. 2. Schematic of the frequency-locking system.

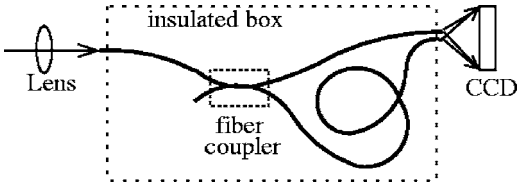

Fig. 3. Schematic of the fiber-optic pinhole interferometer used to provide short-term laser frequency measurements.

sound (5759 m/s) in pure silica presented by Yu *et al.*[13] The exact value of the frequency shift depends on details of fiber construction and temperature.[13]

Figure 2 is a schematic of the frequency-locking system. The laser is a single-longitudinal-mode, frequency-doubled, Nd:YAG laser (Photonics Industries Inc. SLM-DS-10-532). In our HSRL it is operated at low power to provide long pump-diode lifetimes. It provides 40 ns, 250 μJ pulses at a repetition rate of 4 kHz. A wedged beam splitter, WBS1, reflects 4% of the laser light toward a lens that focuses light into a 10 m long, single-mode optical fiber (Fibercore SM450). Stimulated Brillouin light backscattered from the fiber is collimated by the same lens and is directed to wedged beam splitter WBS2. A portion is directed to detector 1, and the rest passes through a 5 cm long I_2 absorption cell and then onto detector 2. Our locking system operates on the pulsed output of the laser. Detectors 1 and 2 are photodiodes followed by integrating circuits that measure the energy in each pulse. Pulse energies are digitally summed for 0.5 s intervals (2000 laser pulses) and then transferred to the data acquisition computer. A simple proportional, integral, differential (PID) servoalgorithm in the data acquisition computer compares the ratio of the signal from detector 2 to the signal from detector 1 with the lock point ratio and corrects the voltage applied to the seed laser frequency tuning input. A scan of the seed laser is used to find the frequency of maximum absorption by line 1109 and the lock point ratio is set at the corresponding value. Because the locking algorithm uses the ratio of the I_2 filtered to unfiltered Brillouin shifted light, it is relatively insensitive to fluctuations in the scattered Brillouin intensity. A servoloop bandwidth of ~0.005 Hz has proven adequate for our application.

Short-term fluctuations in laser frequency are monitored with a fiber-optic pinhole interferometer[14] shown in Fig. 3. A small portion of light from the laser transmitter is focused on the end of a single-mode optical fiber (Fibercore SM450). This light is divided into separate fibers by a 50/50 fiber-optical coupler. Propagation through the unequal length ($\Delta l = 150$ mm) fibers generates a phase delay that depends on the laser frequency. At the output, the fibers are held parallel and epoxied together as closely as possible (~125 μm). Light emitted from the two fibers projects an interference pattern onto a CCD. A frame grabber in the data acquisition computer captures an image of the fringe pattern at 0.5 s intervals. A Fourier transform is applied to one line of 768 pixels oriented across the 33 fringes imaged by the CCD. The phase of the transform is used to track frequency changes. The calibration (218 MHz/rad) is determined by scanning the laser frequency and relating the measured phase shift to the known frequency separation between I_2 absorption features. A one-pixel elongation or compression of the pattern corresponds to a frequency shift of 0.28 MHz. To slow thermal drift, the interferometer is housed within a solid aluminum block that is insulated with two layers of foam and aluminized foil. This interferometer allows precise measurement of relative frequencies measured within a few minutes of one another. Even though the entire lidar is housed in a temperature controlled box (~1°C), thermal drifts (~100 MHz/h) preclude long-term measurements.

Figure 4 shows the Brillouin-shifted transmission of line 1105 as the laser is tuned across line 1109. The frequencies are plotted relative to the frequency where the laser encounters maximum absorption in line 1109. A linear fit to the absorption curve shows that the transmission at the lock point varies at a rate of $-0.7255\ \mathrm{GHz}^{-1}$. Figure 5 shows a 5.5 h record of frequency deviations from the lock point. The lidar temperature was allowed to drift to induce frequency changes. The difference between the reference cell transmission and the lock-point transmission has been divided by the slope of the transmission versus the frequency curve to compute frequency deviations. The standard deviation of the frequency measured here is 18.7 MHz and is mostly due to rapid fluctuations caused by imperfections in the piezo control of the laser cavity length. These are not appreciably damped by the frequency-locking servo. When a 2 min running mean is applied, the standard deviation is reduced to 5.2 MHz.

In normal operation, the Brillouin fiber and the reference cell are temperature controlled to ~1°C to

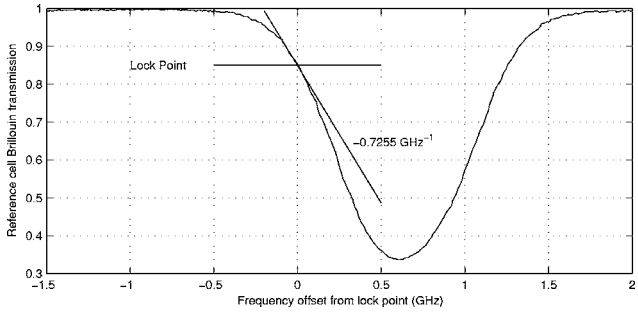

Fig. 4. Reference cell transmission of Brillouin-shifted light by line 1105 as a function of the laser frequency offset from the center of line 1109. Frequency measurements are derived from the interferometer. The I_2 lock-point transmission is shown along with the slope of the transmission curve at the lock point.

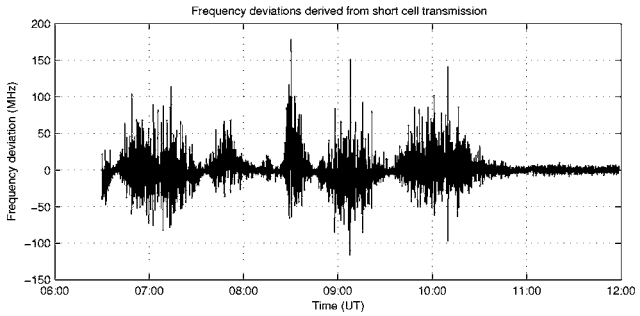

Fig. 5. Frequency deviations of the transmitted laser pulses (2.5 s averages) for a 5.5 h period.

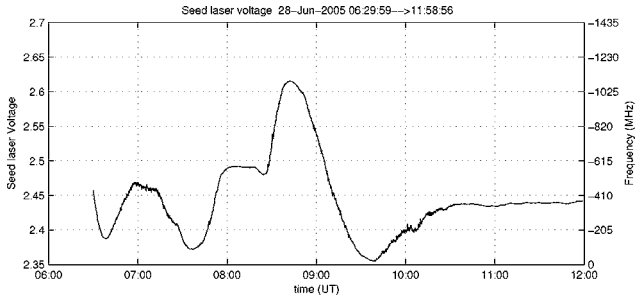

Fig. 6. Voltage feedback signal supplied to the seed laser to maintain lock for the period shown in Fig. 5. The right-side scale converts voltages into frequencies, using the nominal tuning rate of the seed laser.

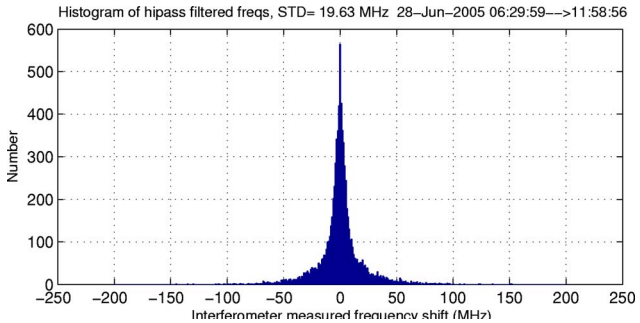

Fig. 7. (Color online) Histogram of frequency deviations from the 100 s mean measured by the interferometer.

reduce errors caused by the temperature dependence of the Brillouin frequency shift ($\sim 1.1 \times 10^{-4}\,^{\circ}\mathrm{C}^{-1}$ or $\sim 3.5\ \mathrm{MHz}\,^{\circ}\mathrm{C}^{-1}$ at 532 nm for pure silica[15]) and changes in the width of the I_2 absorption line ($\sim 24\ \mathrm{MHz}\,^{\circ}\mathrm{C}^{-1}$ for a 5 cm cell at 26°C with free I_2 crystals or $\sim 0.4\ \mathrm{MHz}\,^{\circ}\mathrm{C}^{-1}$ for a starved cell with no crystalline I_2).

Figure 6 shows the voltage applied to the seed-laser tuning input in order to maintain its frequency lock. The right-hand scale converts this into frequency deviations that would occur at the nominal tuning rate of the seed laser. The locking loop nearly eliminates slow changes in the laser frequency; only rapid fluctuations caused by errors in the piezo control of the main laser cavity remain.

Figure 7 provides a histogram of frequency deviations for the period shown in Fig. 5. It shows 2.5 s averaged frequency deviations from the 200 s running median frequency measured with the fiber-optic interferometer. The standard deviation of the frequency is 19.8 MHz. This represents a short-term frequency stability of 3.5×10^{-8} and is dominated by imperfections in the control of the main laser cavity length.

This work was funded by the University Corporation for Atmospheric Research contract S05-39688 and NOAA cooperative agreement NA07EC0676. The frequency-lock software was written by J. P. Garcia. Descriptions of our HSRL can be found at http://lidar.ssec.wisc.edu.

References

1. E. Eloranta, in *Lidar: Range Resolved Optical Remote Sensing of the Atmosphere*, C. Weitkamp, ed. (Springer-Verlag, 2005), pp. 143–164.
2. P. Pirronen and E. Eloranta, Opt. Lett. **19**, 234 (1994).
3. J. Hair, L. Caldwell, D. Krueger, and C. She, Appl. Opt. **40**, 5280 (2001).
4. R. Miles, W. Lempert, and J. Forkey, Meas. Sci. Technol. **12**, R33 (2001).
5. R. Miles, A. Yalin, Z. Tange, S. Zaidi, and J. Forkey, Meas. Sci. Technol. **12**, 442 (2000).
6. P. Schoen and D. Jackson, J. Phys. E **5**, 519 (1972).
7. A. Arie, S. Schiller, E. Gustafson, and R. Byer, Opt. Lett. **17**, 1204 (1992).
8. A. Arie and R. Byer, Appl. Opt. **32**, 7382 (1993).
9. S. Yokoyama, T. Yokoyama, T. Araki, T. Hayashi, and N. Suzuki, Meas. Sci. Technol. **9**, 1252 (1998).
10. P. Pirronen, "A high spectral resolution lidar based on an iodine absorption filter," Ph.D. dissertation (University of Joensuu, 1994).
11. S. Gerstenkorn and P. Luc, *Atlas du spectre d'absorption de la molecule d'iode* (Centre National de la Recherche Scientifique, 1978).
12. J. Forkey, "Development and demonstration of filtered Rayleigh scattering—a laser based flow diagnostic for planar measurement of velocity, temperature, and pressure," Ph.D. dissertation (Princeton University, 1996).
13. J. Yu, Y. Park, and K. Oh, Opt. Express **10**, 996 (2002).
14. T. Pennington, A. Wang, and H. Xiao, Opt. Express **6**, 196 (2000).
15. A. Pine, Phys. Rev. **185**, 1187 (1969).